Probing Enzymatic Activity Inside Single Cells

Jessica Olofsson, Shijun Xu, Gavin D. M. Jeffries, Aldo Jesorka, Helen Bridle, Ida Isaksson, Stephen G. Weber, and Owe Orwar

Supporting Information (SI)

Table of Contents

Supporting Figures

Supporting Figure 1 –Illustration of the Steps for Single-cell Titration

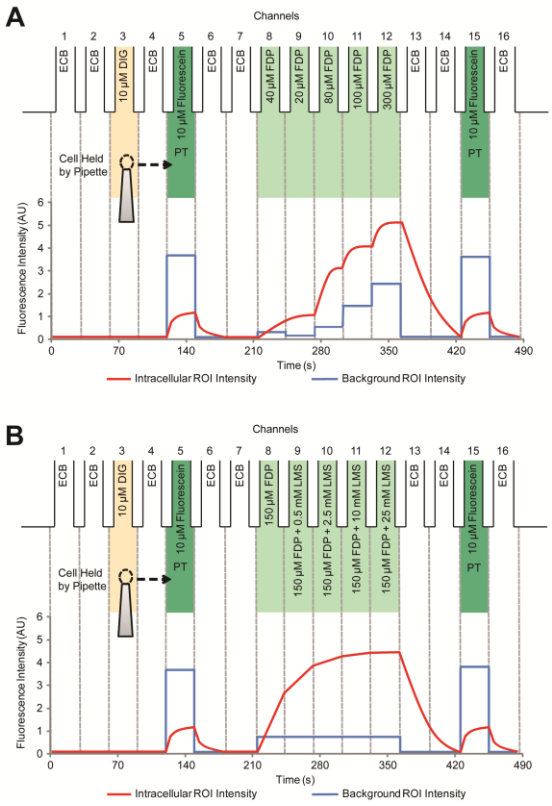

Figure S1. Schematic illustration of the chemical exposure steps used for single cell titration. Two distinct experimental styles were used; (**A**) varying the concentration of the substrate FDP and (**B**) varying the amount of levamisole inhibitor. The upper section of each panel shows the 16 channel outlets of the microfluidic device (DF16 – Cellectricon). Each channel is 50 µm wide and is separated by a 20 µm wide wall. Channels 8-12 were loaded specifically for the experiment style. The other channels were equivalent in all experiments, namely: channels 1, 2, 4, 6, 7, 13, 14 and 16 were loaded with extra cellular buffer (ECB); channels 5 and 15 were loaded with 10 µM fluorescein, as a poration testing (PT)/calibration region; and channel 3 was loaded with 10 µm digitonin (DIG) as the poration agent. For interrogating the FDP dose response, channel 8-12 were loaded with different concentrations of FDP: 40, 20, 80, 100, and 300 and 500 µM respectively. For the inhibition investigation, channels 8-12 were loaded with 150 or 20 µM FDP containing varying concentration of levamisole inhibitor (LMS), 0, 0.5, 2.5, 10 and 25 mM respectively. The procedure is outlined from left to right, whereby a cell held by a patch pipette is translated between the hydrodynamically confined solution environments created at the channel outlets, exposing the cell to well defined chemical environments, for the chosen durations. The lower section of each panel shows a schematic of an experimental curve.

Supporting Figure 2 – 3D Fluorescence Analysis of a NG108-15 Cell

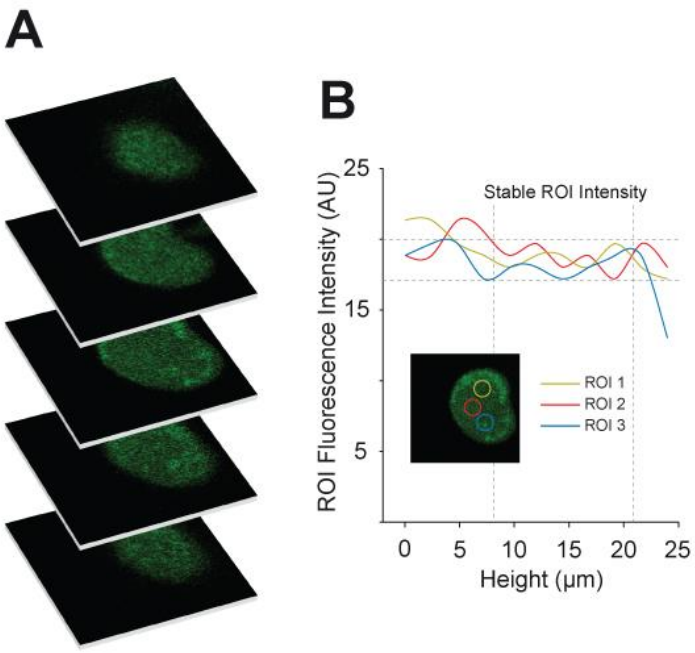

Figure S2. Nature of confocal sectioning effects on ROI analysis. Control tests were performed to ensure that focal height variances and internal local accumulation of fluorescein did not substantially affect the ROI analysis. **(A)** Extracts from an XYZ confocal scan of a fluorescein loaded NG108-15 cell. Fluorescence intensity is well distributed within the cell, and for the ROI size chosen, no significant variances (<15%) were measured within the central 12 μm z-height. **(B)** Three distinct lateral ROI positions (**B** inset) were tested and an equally stable intensity distribution was measured. Together, these indicate that variances in ROI analysis location, both lateral and axial, have minimal impact when chosen about the cell centroid.

Supporting Figure 3 – Measurement Points for Rate Determination

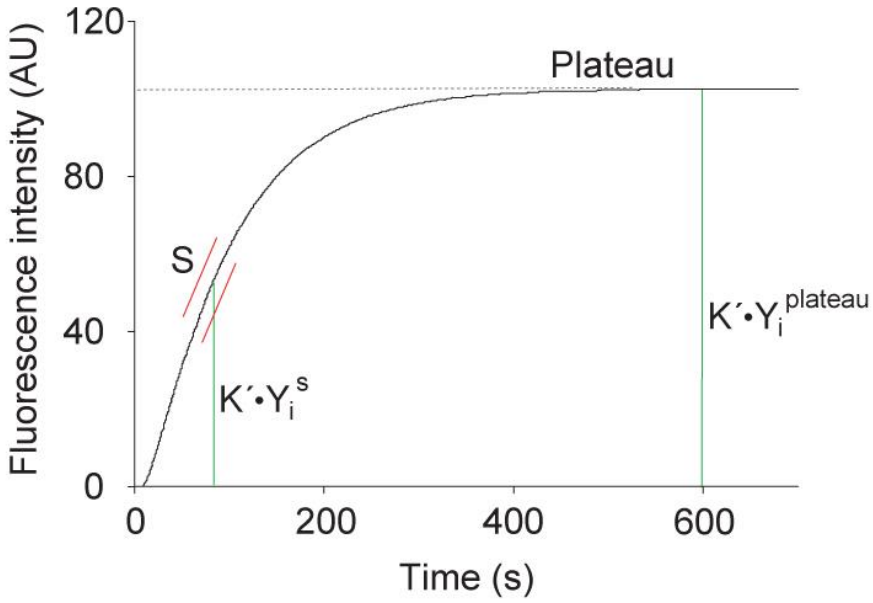

Figure S3. A graphical representation of the measurement points for determination of rate of product formation. A representative curve of intracellular product concentration is displayed as it approaches a steady-state, referred to as a "plateau". S denotes a slope along the curve and is shown bound by red lines on either side of the curve; K´ is a proportionality constant relating fluorescence intensity to intracellular product concentration (see equation (14)); Y_i^S denotes the concentration for the mid-point in the time interval where S is measured. $Y_i^{plateau}$ is the concentration at which a stable plateau is reached.

Supporting Figure 4 – Display of Gradient Measure Points for Varying Product Formation Rates

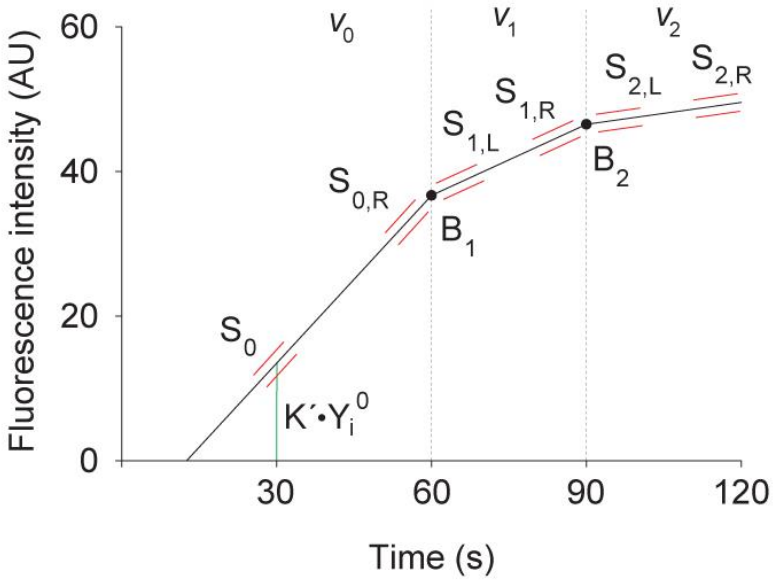

Figure S4. A schematic illustration of how the slopes were measured for varying product formation rates, denoted by v_0, v_1 and v_2. The slopes measured are shown bound by red lines on either side of the curve. S_0 and $S_{0,R}$ (index R stands for right) denote the slopes that will be used as a measure of v_0; $S_{1,L}$ (index L stands for left) and $S_{1,R}$ the slopes that will be used as a measure of v_1; $S_{2,L}$ and $S_{2,R}$ the slopes that will be used as a measure of v_2. B_1 and B_2 denote rate change breakpoints due to a change of substrate or inhibitor concentrations, resulting in changes of v. Finally, Y_i^0 denotes the concentration for the mid-point in the time interval where S_0 is measured and K´ is the proportionality constant relating product concentration and fluorescence intensity.

Supporting Figure 5 – Theoretically Predicted Levamisole Inhibition Degrees for 20 µM and 150 µM FDP Concentration

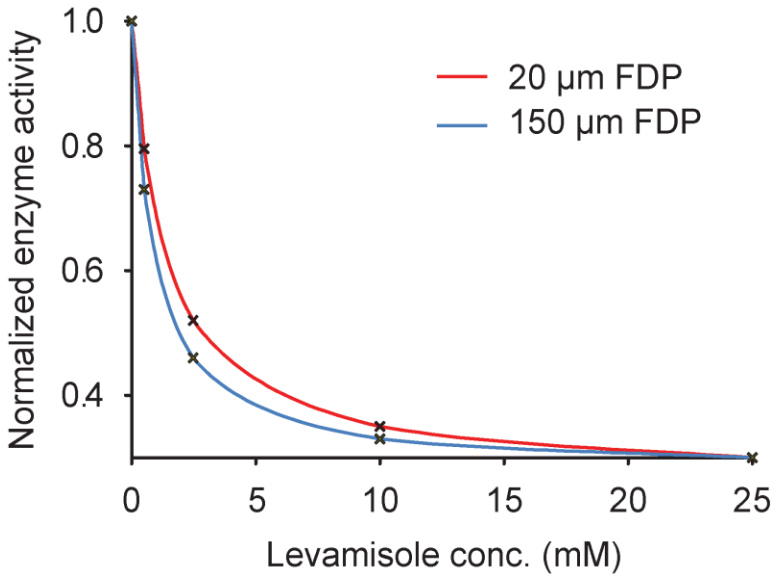

Figure S5. Theoretical dose-inhibition curves for levamisole at two different substrate concentrations. The red and blue curves represent 20 and 150 µM FDP concentration respectively. Curves were produced as described in **Supporting Note 6**, assuming K_m=15.3 µM and K_i= 0.59 mM (average K_m and K_i values obtained from single-cell experiments). Crosses mark the values for 0.5, 2.5, 10 and 25 mM levamisole, the inhibitor concentrations used in experimental measurements.

Supporting Figure 6 –Single Cell Dose Response Plots, Showing the Individual Traces that Compose Figure 3.

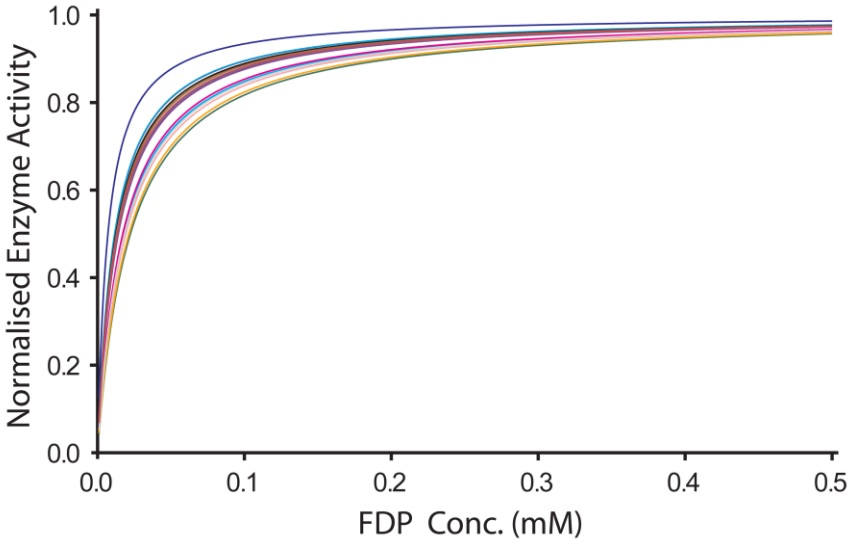

Figure S6. Dose-response plots for alkaline phosphatase within individual NG108-15 cells, used to compose **Figure 3**. Cells were titrated with; 20, 100, 300 and 500 µM FDP or; 20, 80, 100 and 300 µM FDP and the increase in rate of product formation was measured via ROI analysis of confocal microscopy images. The data for each cell was normalized to the highest measured rate of product formation for that cell and fit using Michaelis Menten kinetics to estimate K_m values for alkaline phosphatase within individual cells.

Supporting Figure 7 –Single Cell Dose Inhibition Plots, Showing the Individual Traces that Compose Figure 5.

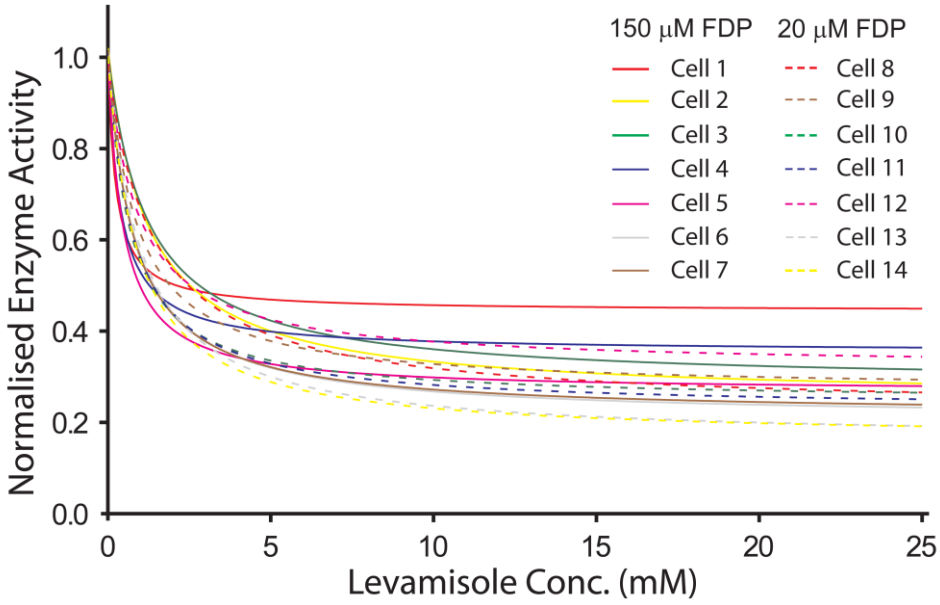

Figure S7. Single cell dose inhibition plots for levamisole, used to compose **Figure 5**. Cells were exposed to either 150 μM FDP or 20 μM FDP and varying levamisole concentrations (0, 0.5, 2.5, 10, and 25 mM). The data for each cell was normalized to the highest measured rate of product formation for that cell and then fit using Michaelis Menten kinetics to allow for extraction of K_i values.

Supporting Figure 8– Bulk Cells Dose-response Plots of Phosphatase for FDP.

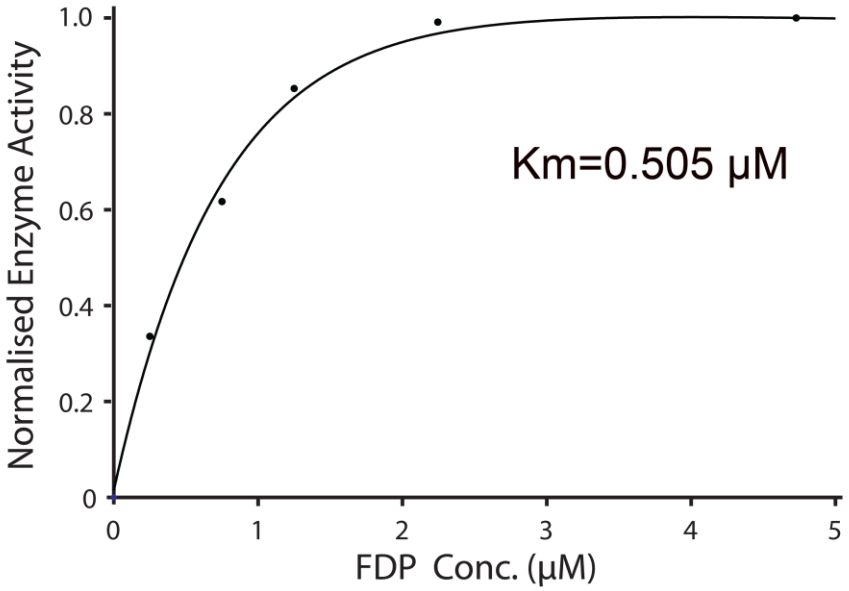

Figure S8. Dose-response plots for phosphatase activity from NG108-15 cells, measured from a digitonin exposure preparation in bulk, using a cuvette. A solution of permeabilized cells was titrated with different concentrations of FDP (0.25, 0.75, 1.25, 2.245 and 4.4728 μM) and the rate of product formation was measured using fluorescence spectrometry. The resulting dose-response data was normalized to the highest product formation rate. Michaelis-Menten kinetics were assumed resulting in a K_m of 0.505 μM. The presented plot shows the data for the mean value K_m, taken from 2 separate experimental series, with further details outlined in **Supporting Note 8**.

Supporting Figure 9– Average Dose-response Plot Constructed from Levamisole Experiments on Bulk Cells.

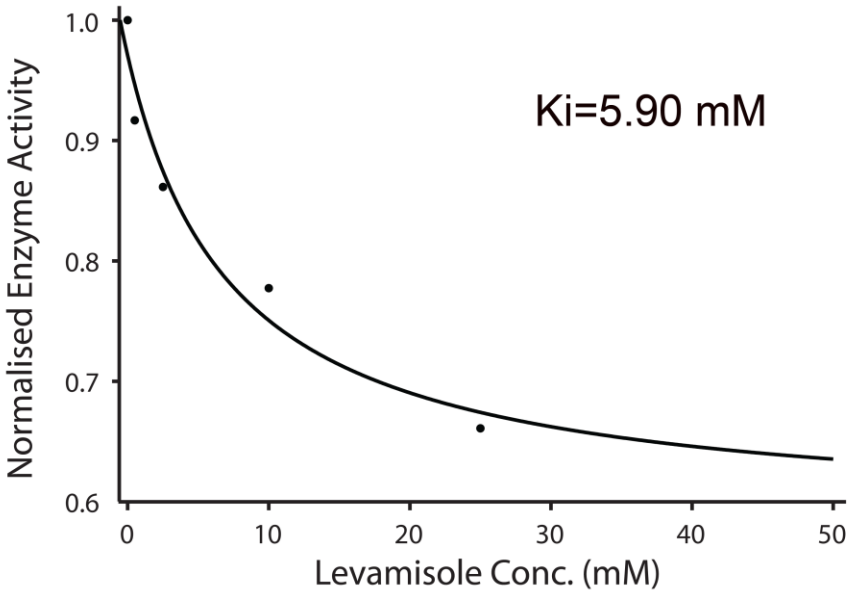

Figure S9. Average dose-response plot constructed from levamisole experiments on porated bulk cell samples (Prepared in similar manner to Fig. S8). Cells were titrated with 20 µM FDP and varying levamisole concentrations (0, 0.5, 2.5, 10 and 25 mM). The data was normalized to unity at the highest concentration and the apparent inhibition constant was extracted from the bulk cell dose inhibition plot. The presented plot shows the data for the mean value K_i (taken from 2 separate experimental series) as an inhibition response chart, with the overlaid curve corresponding to a fit using Michaelis-Menton kinetics. Details are outlined in **Supporting Note 9**).

Supporting Figure 10– Measured Response of Confocal Microscopy to Varying Concentration of Fluorescein in Single Cell.

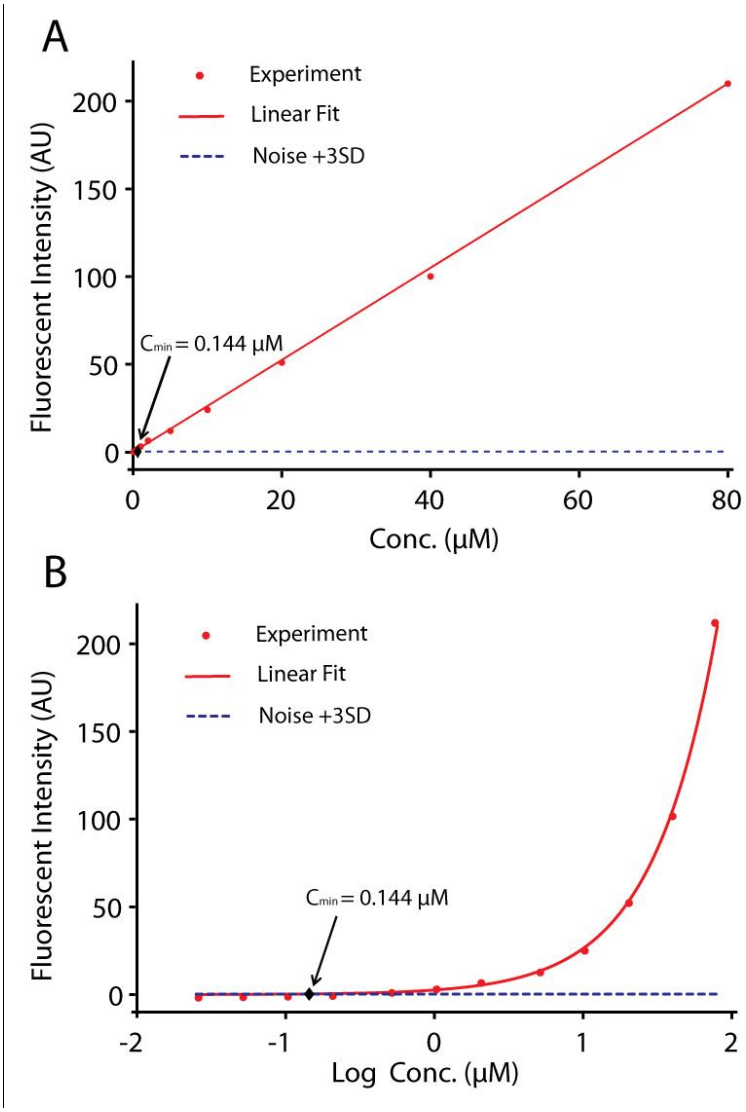

Figure S10. Determination of the limit of detection and dynamic range of confocal microscopy using the single cell interrogation method outlined for the enzymatic analysis. Fluorescence intensity within single cells was measured using the experimentally configured confocal microscope, at varying internal concentrations of fluorescein (0.05-80 µM). Fluorescein concentrations are distributed on a linear scale (A), highlighting the linear relation between intensity and concentration (important in classification as within the linear range of the equipment) and on log scale (B), to more clearly identify the minimum statistically decipherable concentration. The red dots represent the measured fluorescence intensity values for determination of the dynamic range and the fidelity of the measurement. The blue dash line shows the background plus three times maximum of standard deviation, taken as the lowest detectable single concentration change (Details are outlined in **Supporting Note 10**).

Supporting Figure 11– Examine the presence of protein tyrosine phosphatase(PTP) in NG cell.

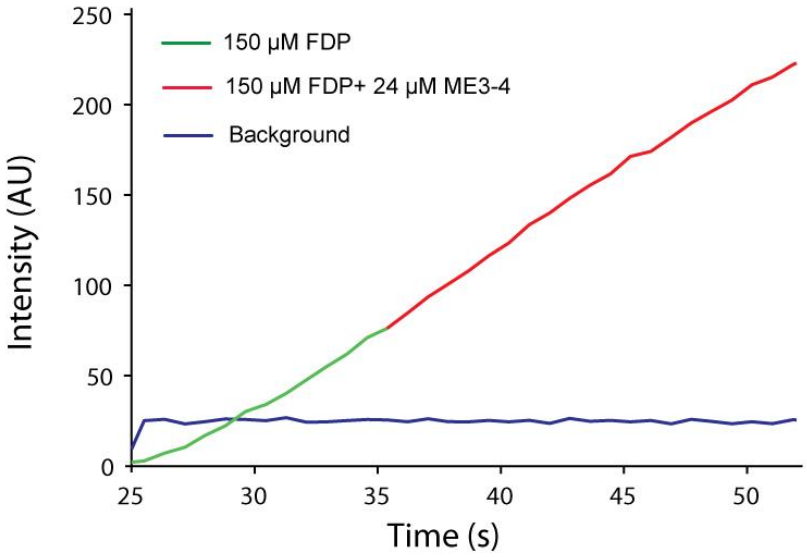

Figure S11. Examining the presence of protein tyrosine phosphatase (PTP) within NG108-15 cells. Methyl-3,4-dephostatin (ME3-4), a typical inhibitor for PTP (k_i=1.6 μM)[1], was used to examine the presence of PTP. The blue curve is extracted from extracellular volume signal, while the green and red line separately represents intracellular enzymatic reaction before and after adding ME3-4. The absence of any gradient change indicates that there is little or no PTP in NG108-15 cell.

Supporting Notes

Supporting Note 1: Theoretical Model for Mass Transport through the Cell Membrane

When a permeabilized cell is placed in an environment containing substrate molecules (*e.g.* FDP), diffusion into the cell will occur, provided that the size of the hydrated substrate is small enough to pass through the pores in the cell membrane. In our model we make the following assumptions:

1. Mass transport is limited by diffusion through the membrane pores. We empirically determined that for the typical conditions (pore densities etc.) used here, on the order of ten seconds is required for the intracellular concentration to reach 90% of its equilibrium concentration when a cell is rapidly moved into a solution containing fluorescein. This equilibration process is a convolution of mass transport to the pores, mass transport through the pores, and intracellular mass transport. Outside the cell there is a convective flow continuously exchanging the solution around the cell on a timescale of 100 ms or less[1]. The convective flow thus provides mass transport to the pores much faster than accumulation inside the cell. The intracellular diffusional relaxation time can be estimated as $r^2/4D_Q$, where r is the cell radius and D_Q the FDP intracellular diffusion coefficient[2]. Assuming a free cell radius of 10 µm and an intracellular diffusion coefficient of $1.5\text{x}10^{-10}$ m^2s^{-1} (estimated as 25% of the corresponding value for bulk diffusion)[3], the intracellular relaxation time is on the order of 100 ms, much shorter than the time required for the intracellular concentration of fluorescein to reach 90% of its equilibrium concentration. These conditions both strongly indicate that the mass transport is primarily governed by diffusion through the membrane pores. The fluid flow about the cell is sufficiently high in volumetric flow-rate to ensure that there is effectively no concentration build-up of product outside the cell, establishing and maintaining an effective external product concentration of zero. On the same basis, a constant external concentration of substrate can be assumed.

2. The flow of molecules through the pores is proportional to the concentration difference across the cell membrane. This assumption is supported by literature[4] and was confirmed *a posteriori*. The fluorescence increase in cells, when exposed to fluorescein during the permeabilization tests, fit well to the exponential equation that was derived based on the above assumption (equation (50)). Further, if the transport of molecules through the pores would occur at a constant rate controlled by the pores rather than being concentration dependent, any addition of substrate molecules above the concentration yielding the highest enzyme activity, would lead to a corresponding increase in intracellular fluorescence. This would occur as the diffusion of product out of the cell would decrease in the competition with the increase of substrate molecules. This was never seen, which further supports our assumption about concentration dependent transport through the pores for our experimental conditions.

Based on these assumptions, the diffusive current I_X (mol/s) of substrate into the cell can be written as

$$I_X = P_{mem,X}A(X_e - X_i) = E_{mem,X}\left(X_e - X_i\right), \qquad (1)$$

where $P_{mem,X}$ (m/s), is the permeability coefficient of the porated membrane with respect to the substrate, A (m^2) is the surface area of the cell, $E_{mem,X} = P_{mem,X}A$ (m^3/s), is a coefficient related to the diffusion of substrate over the cell membrane, X_e (mol/m^3) is the bulk extracellular substrate concentration, and X_i (mol/m^3) is the intracellular substrate concentration.

Upon entering the cell, the substrate (FDP) is enzymatically cleaved into product (fluorescein), primarily by alkaline phosphatase, with a stochiometric ratio of 1:1. We denote the cellular rate of substrate

consumption/product formation by *v* (mol/s). Summing up the contributions to changes in the intracellular substrate concentration we get

$$\frac{dX_i}{dt} = \frac{1}{\alpha V}(-v + I_X), \tag{2}$$

where *V* is the volume occupied by the cell in space, and α is the fraction of this volume that is accessible for substrate and product molecules. Substituting equation (1) into equation (2) we obtain

$$\frac{dX_i}{dt} = \frac{1}{\alpha V}\left(-v + P_{mem,X}A(X_e - X_i)\right). \tag{3}$$

The product accumulation within the cell will drive diffusive transport of product across the membrane. With inward mass transport taken as positive, the flow of product can be written as

$$I_Y = -P_{mem,Y}AY_i = -E_{mem,Y}Y_i, \tag{4}$$

where $P_{mem,Y}$ is the permeability coefficient of the membrane with respect to the product, $E_{mem,Y} = P_{mem,Y}A$ is a coefficient related to the diffusion of product over the cell membrane (analogous to $E_{mem,X}$) and Y_i is the intracellular product concentration. The extracellular product concentration is assumed to be zero, as stated above.

The derivative of the intracellular product concentration per unit time is proportional to the sum of product formation and product loss through diffusion,

$$\frac{dY_i}{dt} = \frac{1}{\alpha V}(v + I_Y). \tag{5}$$

Substituting equation (4) into equation (5) we obtain

$$\frac{dY_i}{dt} = \frac{1}{\alpha V}(v + I_Y) = \frac{1}{\alpha V}\left(v - E_{mem,Y}Y_i\right). \tag{6}$$

As shown in equation (4), diffusion out of the cell is proportional to the intracellular product concentration Y_i. Thus, as Y_i increases, the magnitude of I_Y increases. Eventually, the intracellular product concentration is sufficiently high, that the loss of product by diffusion is balanced by the enzymatic turnover of substrate molecules; thus the concentration of product inside the cell has reached a steady-state $dY_i/dt = 0$, hereafter referred to as a plateau. Substituting $dY_i/dt = 0$ into equation (5) and (6) gives

$$v = -I_Y^{plateau} \tag{7}$$

and

$$v = E_{mem,Y}Y_i^{plateau}, \tag{8}$$

where the index "*plateau*" indicates that a steady-state value is considered, $I_Y^{plateau}$ is the steady state diffusive current of product over the cell membrane, and $Y_i^{plateau}$ is the steady state intracellular product concentration. **Supporting Figure 3** shows a plot of how the intracellular product concentration reaches a plateau. The slope of the curve, S, at any point in time represents the derivative of the intracellular product concentration ($S = dY_i/dt$). As we are utilising a fluorescent product, S can be measured as a change in fluorescence intensity per unit time.

Supporting Note 2: Steady-state Concentrations of Intracellular Substrate and Product

When a permeabilized cell is continuously supplied with substrate, and the intracellular enzymatic reactions are allowed to proceed undisturbed, the intracellular substrate and product concentrations will reach a steady state. For steady-state conditions within the cell, *i.e.* when $dX_i/dt = 0$ and $dY_i/dt = 0$, the consumption of substrate, the formation of product, the flow of substrate into the cell, and the flow of product out of the cell are all of equal magnitude. In this case

$$v = E_{mem,Y} Y_i^{plateau} \tag{9}$$

and

$$v = E_{mem,X}(X_e - X_i^{plateau}). \tag{10}$$

Equating (9) and (10) allows us to write

$$X_i^{plateau} = X_e - \frac{E_{mem,Y}}{E_{mem,X}} Y_i^{plateau} \ . \tag{11}$$

Considering the similar molecular structure of fluorescein and FDP, we assume that their diffusion characteristics are the same, $E_{mem,X} = E_{mem,Y} \circ E_{mem}$, to arrive at a relation between the intracellular substrate and product concentrations at steady-state;

$$X_i^{plateau} = X_e - Y_i^{plateau}. \tag{12}$$

Rearranging equation (10), we obtain

$$X_i^{plateau} = X_e - \frac{v}{E_{mem}}. \tag{13}$$

From equation (12) and $X_i^{plateau} = X_e - \frac{v}{E_{mem}}$. (13) it follows that a low v and a high E_{mem} will give an intracellular substrate concentration X_i that is close to the extracellular substrate concentration X_e, while the intracellular product concentration Y_i will be comparatively low. Conversely, a high v and a low E_{mem}, result in an intracellular product concentration close to the extracellular substrate concentration, while the intracellular substrate concentration will be comparatively low.

Supporting Note 3: Quantification of Relative Changes in Product Formation, through Comparison of Intracellular Steady-state Fluorescence Intensities

The intracellular fluorescence intensity (after background subtraction) is proportional to the intracellular product concentration

$$F_i = K' Y_i, \tag{14}$$

where F_i is the intracellular fluorescence intensity and K' is a proportionality constant.

Substituting equation (14) into equation (9), and exchanging $E_{mem,Y}$ for E_{mem} , results in

$$v = \frac{E_{mem} F_i^{plateau}}{K'}, \tag{15}$$

where $F_i^{plateau}$ is the intracellular fluorescence intensity value at steady-state. If a change in v occurs, as a result of titration with increased substrate or inhibitor concentration, a new steady state concentration, and concomitantly, a new intracellular steady-state fluorescence intensity will be established. To account for this eventuality, we rewrite equation (15) as

$$v_n = \frac{E_{mem} F_i^{plateau,n}}{K'}, \tag{16}$$

where the index n represents different experimental conditions resulting in different product formation rates.

Employing equation (16) we can quantify relative changes in v following changes in experimental conditions according to

$$\frac{v_{n-1}}{v_n} = \frac{F_i^{plateau,n-1}}{F_i^{plateau,n}}, \tag{17}$$

where v_{n-1} and v_n are two different product formation rates, and $F_i^{plateau,n-1}$ and $F_i^{plateau,n}$ are the respective fluorescence intensity plateau values.

Supporting Note 4: Quantification of Relative Changes in Product Formation through Comparison of Fluorescence Intensity Curve Slope Values

The slope S of the fluorescence intensity curve (see **Supporting Figure 3**) at any point in time represents the derivative of the fluorescence intensity (dF_i/dt) and the derivative of the intracellular product concentration (dY_i/dt) according to;

$$S = \frac{dF_i}{dt} = K' \frac{dY_i}{dt}. \tag{18}$$

Another example of this dependency is displayed in **Supporting Figure 4**, presenting a Matlab-simulation for conditions similar to those in **Supporting Figure 3**, except that the product formation rate v is reduced at the 60 and 90 s time points.

Changes in the experimental condition that affect the product formation rate v will affect the rate of product build up and thereby the slope of the curve. Therefore, changes in v can be quantified from alterations in the slope of the fluorescence intensity curve. To estimate the extent to which v is altered due to the changes in experimental conditions, we first define the breakpoints B_n (see **Supporting Figure 4**) on the measured fluorescence intensity curve, where the change is imposed. The slope of the curve is then calculated directly before and after each breakpoint B_n, so that the intracellular concentration of product and the diffusion of product from the cell can be considered quasi-static, during the interval across the two slopes. We call those slopes $S_{n-1,R}$ or $S_{n,L}$ according to which rate (n or n-1) they describe and whether they are in the right (R) or left (L) part of the interval for the rate they describe. The slope $S_{n-1,R}$ is measured just before break point B_n, and $S_{n,L}$ is measured just after break point B_n (see **Supporting Figure 4**). Inserting equation (5) into equation (18) we can then describe the slopes as

$$S_{n-1,R} = \frac{K'}{aV}(v_{n-1} + I_{Y,n-1,R}) \tag{19}$$

and

$$S_{n,L} = \frac{K'}{aV}(v_n + I_{Y,n,L}), \tag{20}$$

where v_{n-1} and v_n is the product formation rates, and $I_{Y,n-1,R}$ and $I_{Y,n,L}$ are the diffusive currents of product out of the cell for the part of the curve where the slope $S_{n-1,R}$ or $S_{n,L}$ is calculated, respectively.

Defining a new proportionality constant,

$$K \circ \frac{K'}{aV} \tag{21}$$

and substituting into equation (19) and equation (20) we obtain

$$S_{n-1,R} = K(v_{n-1} + I_{Y,n-1,R}) \tag{22}$$

and

$$S_{n,L} = K(v_n + I_{Y,n,L}). \tag{23}$$

As we assume the diffusion out of the cell to be quasi-static during the intervals around a breakpoint, where the slopes $S_{n-1,R}$ and $S_{n,L}$ are estimated, we can write

$$I_{Y,n,L} = I_{Y,n-1,R} + E_n^{nr1}, \tag{24}$$

where E_n^{nr1}, defined as the difference between $I_{Y,n,L}$ and $I_{Y,n-1,R}$. The experiment should be designed so that is small, so that it can be neglected in the equations. Defining Δ_n as the difference between $S_{n-1,R}$ and $S_{n,L}$ and using equation (22), equation (23), and equation (24) we can write;

$$\Delta_n \equiv S_{n-1,R} - S_{n,L} = K(v_{n-1} - v_n - E_n^{nr1}). \tag{25}$$

Equation (25) can be rearranged to

$$v_{n-1} - v_n = \frac{\Delta_n}{K} + E_n^{nr1}. \tag{26}$$

If the proportionality constant K is known and E_n^{nr1} neglected, equation (26) can be used to estimate the difference between v_{n-1} and v_n in absolute terms. For the case that K is not known, we now establish a method to estimate the difference between v_{n-1} and v_n relative a reference product formation rate v_0 which is the rate at an initially established reference condition. To achieve this, a known relation between v_0 and a measurable slope S of the fluorescence intensity curve is required. Inserting equation (5) into equation (18) and substituting v for v_n (to account for the possibility of different experimental conditions represented by the index n), we obtain

$$S = K' \frac{v_n + I_Y}{aV}. \tag{27}$$

Further, exchanging $E_{mem,Y}$ for E_{mem} in equation (4) and combining with equation (14), we can express the flow of product over the cell membrane as a function of the intracellular fluorescence intensity as

$$I_Y = -E_{mem} Y_i = -\frac{E_{mem} F_i}{K'}. \tag{28}$$

The ratio between an arbitrary I_Y and the diffusive current out of the cell at a plateau n, $I_Y^{plateau,n}$, is then

$$\frac{I_Y}{I_Y^{plateau,n}} = \frac{F_i}{F_i^{plateau,n}} \tag{29}$$

where $F_i^{plateau,n}$ is the intracellular fluorescence intensity at steady state. Assuming a steady state intracellular product concentration, $dY_i/dt = 0$, we can use equation (5) to write

$$I_Y^{plateau,n} = -v_n. \tag{30}$$

We can express the diffusion of product over the cell membrane in terms of v_n by inserting equation (30) into equation (29). Rearranging, this yields

$$I_Y = -v_n \frac{F_i}{F_i^{plateau,n}}. \tag{31}$$

Inserting equation (31) into equation (27) now gives

$$S = \frac{K' v_n}{aV}\left(1 - \frac{F_i}{F_i^{plateau,n}}\right). \tag{32}$$

Inserting equation (21) into equation . (32) and choosing n=0 now leads to

$$S_0 = K v_0 \left(1 - \frac{F_i^0}{F_i^{plateau,0}}\right), \tag{33}$$

where S_0 is the slope measured to represent the product formation rate at the reference condition v_0, F_i^0 is the fluorescence intensity of the curve where S_0 is measured, and $F_i^{plateau,0}$ is the fluorescence intensity at steady state for the reference product formation rate v_0.

Dividing equation (25) with equation (33) we obtain

$$\frac{\Delta_n}{S_0} = \frac{S_{n-1,R} - S_{n,L}}{S_0} = \left(v_{n-1} - v_n + E_n^{nr1}\right) \Big/ \left[v_0 \left(1 - \frac{F_i^0}{F_i^{plateau,0}}\right)\right] \tag{34}$$

which when rearranged finally allows for v_n/v_0 to be estimated iteratively from v_{n-1}/v_0 as

$$\frac{v_n}{v_0} = \frac{v_{n-1}}{v_0} - \left(1 - \frac{F_i^0}{F_i^{plateau,0}}\right)\frac{\Delta_n}{S_0} + \frac{E_n^{nr1}}{v_0} = \frac{v_{n-1}}{v_0} - \left(1 - \frac{F_i^0}{F_i^{plateau,0}}\right)\frac{(S_{n-1,R} - S_{n,L})}{S_0} + \frac{E_n^{nr1}}{v_0}\ . \tag{35}$$

For example, for n = 1,2 this yields

$$\frac{v_1}{v_0} = \frac{v_0}{v_0} - \frac{\left(1 - F_i^0/F_i^{plateau,0}\right)\left(S_{0,R} - S_{1,L}\right)}{S_0} + \frac{E_1^{nr1}}{v_0} = 1 - \frac{\left(1 - F_i^0/F_i^{plateau,0}\right)\left(S_{0,R} - S_{1,L}\right)}{S_0} + \frac{E_1^{nr1}}{v_0} \tag{36}$$

and

$$\frac{v_2}{v_0} = \frac{v_1}{v_0} - \frac{\left(1 - F_i^0/F_i^{plateau,0}\right)\left(S_{1,R} - S_{2,L}\right)}{S_0} + \frac{E_1^{nr1}}{v_0} + \frac{E_2^{nr1}}{v_0}, \tag{37}$$

where v_0 is the product formation rate at the reference condition, v_1 is the product formation rate after the first perturbation is imposed and v_2 is the product formation rate after the second perturbation is imposed (see **Supporting Figure 4**). The iterative estimation of different v_n/v_0 described in equation (35) can be condensed into the recursion formula

$$\frac{v_n}{v_0} = 1 - \left(1 - F_i^0/F_i^{plateau,0}\right)\sum_{n'=1}^{n}\frac{\Delta_{n'}}{S_0} + \sum_{n'=1}^{n}\frac{E^{nr1}_{n'}}{v_0} \tag{38}$$

where $\Delta_{n'} = S_{n'-1,R} - S_{n',L}$ and $n' \geq 1$. If the term $F_i^0/F_i^{plateau,0}$ is small compared to 1, that is, if the diffusion of product out of the cell is small compared to v_0 where S_o is measured, equation (38) can be written as

$$\frac{v_n}{v_0} = 1 - (1 - E^{nr2}) \sum_{n'=1}^{n} \frac{\Delta_{n'}}{S_0} + \sum_{n'=1}^{n} \frac{E_{n'}^{nr1}}{v_0}, \tag{39}$$

where

$$E^{nr2} = \frac{F_i^0}{F_i^{plateau,0}} \tag{40}$$

is small compared to 1. Assuming E_n^{nr1} and E^{nr2} to be small enough to be neglected with satisfactory outcome, equation (39) reduces to

$$\frac{v_n}{v_0} \approx 1 - \sum_{n'=1}^{n} \frac{\Delta_{n'}}{S_0}, \text{ where } \Delta_{n'} = S_{n'-1,R} - S_{n',L} \text{ and } n \geq 1. \tag{41}$$

It is possible to estimate the terms E_n^{nr1}/v_0 and E^{nr2}, and thereby the error introduced in v_n/v_0 through neglecting those terms. To this end, the value of $F_i^{plateau,0}$ is required. Either a measurement of $F_i^{plateau,0}$ can be included in the experimental design, or $F_i^{plateau,0}$ can be estimated *a posteriori*, through use of equation (16). Through inserting the height of experimentally measured plateau values ($F_i^{plateau,n}$) and their associated enzymatic activity (v_n), the proportionality constant between enzyme activity and expected plateau height can be calculated, and subsequently used to calculate the expected plateau height for the product formation rate at the reference condition (v_0). When $F_i^{plateau,0}$ is known, E^{nr2} can be estimated using equation (40), as F_i^0 (the fluorescence intensity of the curve where S_0 is measured) is known from the experimental curves. Combining equation (24), which states that E_n^{nr1} is the difference between $I_{Y,n,L}$ and $I_{Y,n-1,R}$, with equation (4) and (14) we can write

$$\frac{E_n^{nr1}}{v_0} = \frac{I_{Y,n-1,R} - I_{Y,n,L}}{v_0} = \frac{F_i^{n-1,R} - F_i^{n,L}}{F_i^{plateau,0}} \tag{42}$$

where $F_i^{n-1,R}$ and $F_i^{n,L}$, are the fluorescence intensities known from the experimental curves for the intracellular product concentrations $I_{Y,n-1,R}$ and $I_{Y,n,L}$.

Supporting Note 5: Estimation of the Number of Pores from Permeability Coefficients

According to Fick´s first law, the flux of molecules (mol/(m^{2}s)) within a concentration gradient is

$$J = -D_Q \nabla Q, \tag{43}$$

where D_Q is the transport diffusion coefficient for the molecule (m^{2}s^{-1}) and Q represents the concentration (mol/m^3). Using Fick´s first law we can express the diffusive current I_p through a circular pore in an otherwise non-permeable cell membrane as

$$I_p = \rho r_p^2 D_Q \frac{(Q_e - Q_i)}{h}, \tag{44}$$

where r_p is the radius of the pore, h is the thickness of the membrane, Q_e is the concentration outside the cell, and Q_i is the concentration inside the cell. The total mass flow through pores in an area A of the cell membrane thus can be expressed as

$$I = NI_p = N\rho r_p^2 D_Q \frac{(Q_e - Q_i)}{h}, \tag{45}$$

where N is the number of pores in the area A. If alternatively expressed in terms of membrane permeability P, the mass transport of molecules over the membrane can be expressed as

$$I = PA(Q_e - Q_i). \tag{46}$$

Equating equations (45) and (46) shows that

$$PA = \frac{N\pi r_p^{\,2} D_Q}{h}, \tag{47}$$

and thus we can obtain an estimate for the number of pores N as

$$N = \frac{PAh}{\pi r_p^2 D_Q}. \tag{48}$$

Using a permeability coefficient of 0.3 µm/s (the upper limit for the cells used in our experimental series), a pore radius of 4 nm, and a transport diffusion coefficient for fluorescein of 1.5×10^{-10} m^2/s (estimated as 25% of the corresponding value for bulk diffusion)[5] gives approximately 15×10^{10} pores per square meter of membrane. For a spherical cell of radius of 10 µm, approximately 200 pores would be expected in total.

The assumption that the transport diffusion coefficient for fluorescein through the pores is 25% of that measured in bulk is based on literature and is a highly variable approximation[5]. If the diffusion coefficient would be as in bulk, the number of pores would be approximately 50. If the diffusion coefficient for fluorescein in the pores would instead be only 5% of its bulk value the number of pores would be approximately 1000. We conclude that the number of pores in a typical cell likely is in the range of 50 to 1000, that is ~100.

Supporting Note 6: Theory Predicts Small Difference Between Inhibition Experiments Using 20 µM and 150 µM FDP

We performed dose inhibition experiments using both 20 µM and 150 µm FDP concentrations. Levamisole is reported to be an uncompetitive inhibitor, and the degree of inhibition is therefore not only dependent on inhibitor concentration but also on substrate concentration. We experimentally observed similar inhibition effects at both 20 µM and 150 µM FDP concentrations, inciting a further investigation into the expected differences.

This was achieved through plotting the theoretical curves predicted as

$$\frac{v}{V_{\max}} = \frac{X_i}{X_i\left(1+Z/K_i\right)+K_m} + B \qquad (49)$$

where V_{max} is the maximum product formation rate, X_i is the intracellular substrate concentration, Z is the concentration of inhibitor, and B is an arbitrary constant. The substrate concentration was set to 20 µM or 150 µM, and K_m vas set to 15.3 µM (the average value obtained from our experiments). B and V_{max} were set so that $v/V_{\max}=1$ for Z=0, and v=0.3 (to resemble experimental curves as given in **Figure 3**) for Z=25 mM. The difference between the theoretical curves for 20 µM and 150 µM is small (**Supporting Figure 5**), which matches very well our experimental findings.

Supporting Note 7: Estimating the Permeability of Porated Cell Membranes

The permeability of the cell membrane was elucidated by translating the cells from pure buffer solution to a solution containing fluorescein, then following how the intracellular concentration equilibrated with the extracellular concentration. The obtained fluorescence intensity curves were expressed as concentrations by fitting to the equation

$$Q = (Q_0 - Q_e)e^{-\frac{AP}{aV}t} + Q_e, \qquad (50)$$

where Q_e is the extracellular concentration and Q_0 is the initial intracellular concentration, P is the membrane permeability coefficient for the considered species, A is the cell surface area, V is the volume occupied by the cell in space, and a is the fraction of this volume that is accessible to fluorescein. In fitting parameters, we assumed $a=1$, Q_0=0 and a spherical cell shape, where the volume of the cell was estimated from bright field images. An overestimation of the fraction of the volume accessible to fluorescein (a) results in a concomitant overestimation of the permeability coefficient of the plasma membrane (see exponent in equation (50)). Therefore, the true permeability coefficient is believed to be smaller than the estimated permeability coefficient for cells that do not reach maximal internal fluorescence intensity. We chose to denote the estimated permeability coefficient as an apparent permeability coefficient. As a further indication of this, we occasionally, upon additional permeabilization of cells, observe a transition to maximal fluorescence intensity in poration tests associated with a decrease in the estimated permeability coefficient P. In those cases we put the decrease in the apparent P in relation to an increase in the accessible volume of the cell (due to decreased molecular crowding as a result of loss of cytosolic components), rather than a decrease in the number of pores.

When the constant a is overestimated, the membrane permeability coefficient P and the related constant E_{mem} also become overestimated. Consequently, using equation (8), (15) or. (32) to estimate the product formation rate v (mol/s) gives an overestimation. However, it is possible to calculate the rate of product formation $\frac{v}{aV}$, where aV is the volume of the cell that is accessible to substrate and product molecules $\frac{v}{aV}$ is the rate of product formation given in units of M/s. In this case, aV does not have to be known (for equation . (32)),

or the errors introduced through using a possibly erroneous value of P or E_{mem} in the calculation is cancelled by the error in a (for equation (8) and (15)).

Supporting Note 8: Bulk Dose-Response measurement of Phosphatase Activity in NG108-15 cells using FDP

Varying concentrations of the substrate FDP (0.25, 0.75, 1.25, 2.245 and 4.4728 µM) were added to a solution of permeabilized NG108-15 cells and the rate of product formation (fluorescein) was monitored using fluorescence spectroscopy (λ_{ex}=488 nm, λ_{em}=512 nm). The solution of cells and FDP were continuously agitated by a magnetic stirrer during the measurement to avoid sedimentation of cells. Supporting Figure 8 shows the resulting dose response plot. The Michaelis constant K_m was calculated to be 0.505 µM.

Supporting Note 9: Inhibition Response for Levamisole in Bulk Cells

The investigation of inhibition of phosphatase activity in NG15-108 cells in bulk for levamisole is determined by the same procedure as described for FDP bulk dose-response measurements (Supporting note 8). Cells were titrated with substrate FDP (20 µM) and the inhibitor **(**levamisole**)** solution with the same concentrations as in single-cell measurements (0, 0.5, 2.5, 10 and 25 µM). Supporting Figure 9 presents a curve of enzyme activity versus inhibitor concentration. An inhibition constant K_i of 5.90 mM was obtained.

Supporting Note 10: Estimating the Sensitivity and Dynamic Range of Confocal Microscopy

To evaluate the sensitivity and dynamic range of our assay, a calibration plot was constructed (see Supporting Figure 10), whereby fluorescein (the enzymatic product) was introduced into the cell at various concentrations, ranging from 0.05 µM to 80 µM. A linear relation between concentration and fluorescence intensity was measured for the entire span of tested concentrations. For the settings used in our experiments 80 µM gave a fluorescence signal close to the limit for detector linearity at approximately 250 AU.

According to the detection limit concept, the minimum detectable signal is given by

$$S_m = S_b + K(Std) \tag{51}$$

where S_m is the minimum detectable analytical signal, S_b is the instrument signal for blank (noise) and *Std* is the standard deviation of the signal for blank. For detection, K is equal to 3.

The basis for the quantitative analysis of concentrations from a measure property is a known relation between the magnitude of the measured property and the concentration. In our case this relation is linear and described by

$$S = a[C] + b \tag{52}$$

where S is the measured signal, a is the slope as decided by a calibration curve, $[C]$ is the analyte concentration and *b* is the intercept of the calibration curve.

Assuming $S = S_m$, the minimum detectable concentration can be calculated as

$$[C]_{\min} = \frac{S_b + K(Std) - b}{a} \quad (53)$$

As depicted in Supporting Figure 10, the mean background value was 0.015707. After a three times noise amplification step, we were able to distinguish concentration as low as 0.144 µM above background.

A cell of 10 µm radius with the volume (V) equal to 4.24×10^{-12} L is assumed. The minimum detectable rate of assay requires 3 data points (with a 10s delay between each measurement) and can be estimated by the following equation:

$$v_{\min} = V(1-D)\frac{[C]_{\min} + 2(3*Std)}{T} \quad (54)$$

where T is the time to achieve the minimum detectable concentration (3 measurements) and D is the fraction of formed product that diffuse out from the cell per unit time.

The maximum rate determination requires the signal to be within the linear range of the detector, while able to measure 3 data points. The maximum concentration was derived from the calibration plot, where detector linearity finishes at approximately 250 AU.

$$v_{\max} = V(1-D)\frac{([C]_{\max} - [C]_{\min})}{2T} \quad (55)$$

Assuming D=0 and using equation (54) for calculation, for a typical FDP and phosphatase reaction, the minimum detectable rate was measured to be 2.0×10^{-20} mol/s, and using equation (55) the maximum measurable rate was determined to be 2.5×10^{-18} mol/s. Under these experimental conditions, the minimum detectable change of rate was calculated to be 0.44×10^{-20} mol/s (derived form 3*Std of the mean signal value).

Supporting Note 11: Determining which enzyme is observed in the NG cell analysis

FDP is a phosphatase substrate particularly suitable for measuring AP and protein tyrosine phosphatase (PTP) activity. In our experiments, the specific AP inhibitor levamisole[6] blocked a major part of the FDP hydrolysis while the PTP specific inhibitor methyl-3,4-dephostatin[7] did not affect the enzyme kinetics (see supporting figure 11). This validates our assumption that most of the observed enzymatic turnover is due to alkaline phosphatase.

References

1. Sinclair, J.; Pihl, J.; Olofsson, J.; Karlsson, M.; Jardemark, K.; Chiu, D. T., Orwar, O. *Anal Chem.* **2002**, *74*, 6133-6138.
2. Crank, J. *The mathematics of diffusion*. 2nd ed. ed. Oxford: Clarendon Press, 1975.
3. Seksek, O.; Biwersi, J., Verkman, A. S. *Journal of Cell Biology.* **1997**, *138*, 131-142.
4. Cui, S. T. *J Chem Phys.* **2005**, *123*.

5. Beck, R. E., Schultz, J. S. *Abstr Pap Am Chem S.* **1970**, 104-&.
6. Cyboron, G. W.; Vejins, M. S., Wuthier, R. E. *J Biol Chem.* **1982**, *257*, 4141-4146.
7. Fujiwara, S.; Watanabe, T.; Nagatsu, T.; Gohda, J.; Imoto, M., Umezawa, K. *Biochem Biophys Res Commun.* **1997**, *238*, 213-217.